

Research Article

A Performance Comparison of Centralized and Distributed Spectrum Management Techniques in Elastic Optical Networks

Tushar Mathur , Gokhan Sahin , and Donald R. Ucci

Electrical and Computer Engineering Department, Miami University, 650 E High St., Oxford, OH, USA

Correspondence should be addressed to Gokhan Sahin; sahing@muohio.edu

Received 12 July 2018; Revised 24 October 2018; Accepted 18 November 2018; Published 1 January 2019

Academic Editor: A. S. Madhukumar

Copyright © 2019 Tushar Mathur et al. This is an open access article distributed under the Creative Commons Attribution License, which permits unrestricted use, distribution, and reproduction in any medium, provided the original work is properly cited.

Elastic optical networks (EONs) have emerged to provide higher spectrum efficiency than traditional Dense Wavelength-Division-Multiplexing (DWDM) by utilizing enabling technologies such as flexible spectrum grid, Orthogonal Frequency Division Multiplexing (OFDM), and distance adaptive rate and modulation. The choice of the control-plane is an important consideration when deploying any new technology, especially in optical networks. This paper considers generic distributed and centralized spectrum assignment policies in conjunction with the accompanying connection set-up signaling protocols in EONs. A network simulator for Generalized Multiprotocol Label Switching (GMPLS) was developed with Forward Reservation Protocol and Backward Reservation Protocol signaling methods. These signaling techniques are used with the First Fit (FF) and Random Fit (RF) Routing and Spectrum Allocation (RSA) algorithms. The paper discusses control elements (central and distributed architectures) decisions under busy hour and normal network conditions and presents a comprehensive performance analysis of key performance metrics such as connection success rate, connection establishment time, and capacity requirement.

1. Introduction

Today's DATA communication networks are growing at a rapid pace (Figure 1). Of late, the Internet caters to end users with different applications, such as high-definition IP videos (Netflix, Hulu, YouTube), file sharing tools (Google Drive, Dropbox), Voice over IP, and fully immersive video technologies such as Virtual Reality. To add to the consumed bandwidth, multiple devices can be used to access Internet content.

Optical networks are the crux of Internet communication technology because of their inherent nature of providing low bit error rates and higher bandwidth capacity. Network traffic trends grow exponentially and there is a need for efficient and flexible optical transport networks that should be able to support multirate and large bandwidth (100s of Gbps to Tbps) connections [1–3]. Currently, Wavelength Division Multiplexed (WDM) networks are widely deployed as backbone Internet networks. WDM networks have been so far able to support fixed granularity interfaces. WDM systems use rigid frequency grids and transmit data at

single bit-rate using single-carrier modulation techniques (Quadrature Amplitude Modulation or QAM).

To sustain the growth of bandwidth capacity, it is essential to have flexible data-rates, multicarrier modulation techniques, and resource efficient spectrum allocation methodologies, as compared to traditional WDM networks. Orthogonal Frequency Division Multiplexing (OFDM) is a special class of multicarrier modulation that can transmit high-speed data streams by dividing the channel into multiple orthogonal subcarriers [1–3], each carrying a relatively low data-rate in parallel. WDM requires a fixed sized guard band between channels to eliminate Inter-Symbol Interference (ISI). The subcarriers in OFDM are overlapped but, despite this overlapping, ISI is mitigated by the longer OFDM symbol duration. The orthogonality and, hence, the overlapping of subcarriers, result in efficient usage of spectral resources.

With OFDM, the bandwidth is flexible and can be broken into strands; i.e., the channel is divided into finer granularity. This system has a technical and an economic advantage. Figure 2 shows the efficient usage of the spectrum by dividing it into multiple subcarriers and data-rates as a function of the

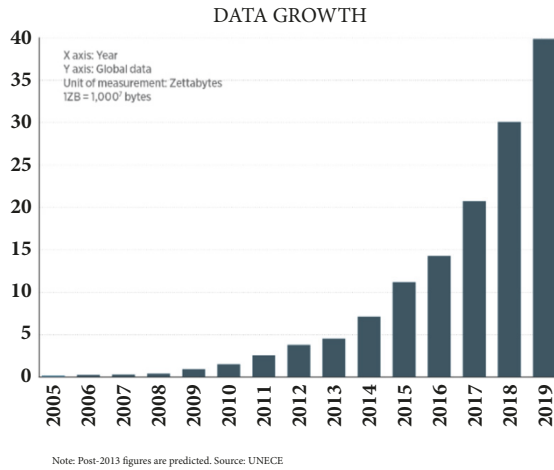


FIGURE 1: The network data growth. Source UNECE.

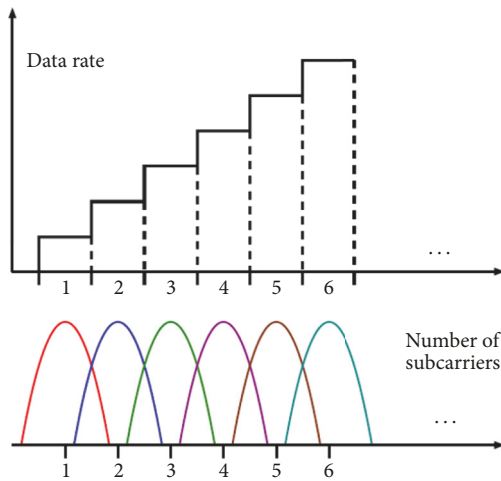


FIGURE 2: Data-rates as a function of number of subcarriers in an OFDM channel. Source [4].

number of subcarriers in a channel. These subcarriers may be used on per demand basis, i.e., the flexibility to change data-rates on a subcarrier assignment to a connection demand type.

To account for the needs of escalating bandwidth demands, an OFDM based network technology is poised to replace the existing rigid WDM spectrum system [1–17]. This technological challenge has propelled the research community to develop a new paradigm in optical network technology, namely, Elastic Optical Networks (EONs) or Spectrum Sliced Elastic Optical Networks (SLICE) [3], or Flexi-Grid Dense WDM (FG-DWDM) Networks that uses OFDM as the underlying physical layer technology. There has been a substantial amount of work already performed on centralized and distributed resource allocation algorithms and signaling protocols designed for improving the performance in EONs [1–17]. Generalized Multiprotocol Label Switching (GMPLS) based signaling protocols and their extensions are

commonly utilized for this purpose [5, 6, 11, 14] following the well-established practice of separating the control-plane and the data-plane in WDM optical networks [18–20]. It is noted that despite the recent interest in applying a Software Defined Networking (SDN) paradigm (e.g., OpenFlow protocols) in optical networks [21, 22] some researchers envision that a traditional embedded control-plane based on GMPLS will continue to be in place even in optical networks that utilize SDN due to factors and performance requirements specific to optical networks [23]. These factors include vendor proprietary frame formats, different granularity of grooming functions, proprietary modulation/encoding and Forward Error Correcting (FEC) schemes, and stringent recovery time constraints [23].

This work provides a detailed performance comparison of distributed and centralized spectrum allocation algorithms in EONs, in conjunction with the accompanying GMPLS-based signaling methods with forward and backward reservation. Realistic case studies for normal network conditions and busy hour traffic are utilized, with consideration of three key performance metrics: connection success-rate (or blocking probability), connection set-up time, and the capacity requirement. This work can serve as a guide for network architects in evaluating the trade-offs involved among the various system options available.

The rest of the paper is organized as follows. Section 2 presents a summary of related work. Section 3 provides background information on EONs and GMPLS-based signaling protocols. Section 4 introduces the routing and spectrum allocation problem and associated algorithms. Section 5 describes the simulation environment. Section 6 provides a performance comparison of various spectrum allocation algorithms under parallel (busy hour) and normal traffic conditions. Section 7 discusses forward and backward signaling methods considering various performance metrics. Section 8 concludes the paper.

2. Related Work

EONs have been extensively studied over the past decade [22, 24–32] from various perspectives [24], from early architectural assessments establishing the potential advantages of EONs over fixed-grid WDM [25] to specific resource allocation studies that aim to provide efficient routing and spectrum allocation algorithms [24, 26, 27] or solutions to the spectrum fragmentation problem in EONs [29]. References [25, 26] cover key aspects of EON or SLICE, i.e., the rules of frequency allocation, reservation mechanism, and routing and spectrum allocation algorithms. The key concepts and enabling technologies for EONs, such as OFDM technology and bandwidth variable optical cross-connects are discussed in [27]. Many studies that deal with signaling aspects have used the basic First Fit and Random Fit spectrum assignment algorithms in their simulations and we borrowed the idea in this paper [29]. Numerous sophisticated routing and spectrum allocation algorithms have been developed that achieve better capacity utilization but require a higher level of processing or complexity including [4, 7, 10, 15, 16, 26, 29, 33]. EON planning using statistical path models is demonstrated

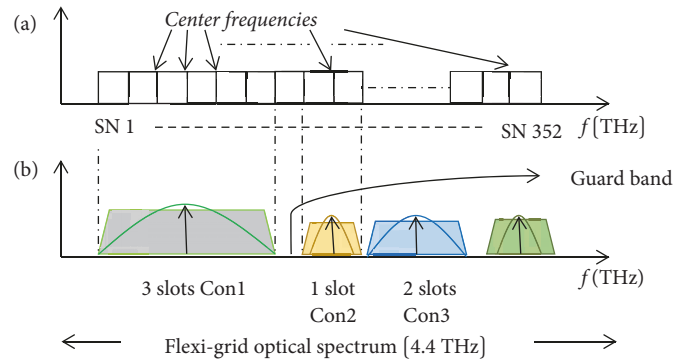


FIGURE 3: Slots in a Flexi-grid network: (a) slots in flexi-grid frequency spectrum have a nominal center frequency granularity of 6.25 GHz, with the slot width of 12.5 GHz; (b) connections 1, 2 and 3 with even number of slots around a center frequency and a guard band between connections 1 and 2.

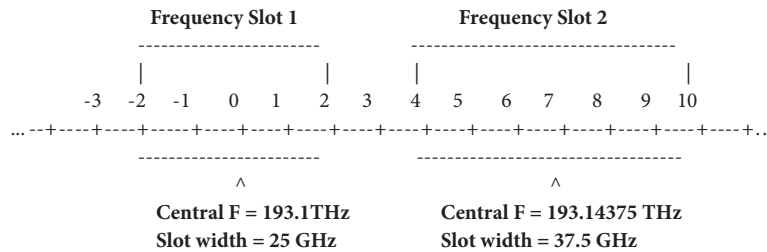


FIGURE 4: Frequency Slot example from the flexi-grid optical network standard [5].

in [30]. We refer the readers to recent surveys and edited volumes for a comprehensive and detailed overview of EON-related research in various dimensions [1, 2, 22, 24, 28]. Our work is inspired by similar comparative studies in WDM networks [19], and is based on the results reported in [31].

We note that both centralized and distributed spectrum management techniques in EONs have their own advantages and challenges [24, 32]. In theory, centralized management can provide more compact capacity utilization and higher connection establishment success rate as it can use optimal or near-optimal spectrum assignment and eliminate all spectrum contentions during the connection set-up process. However, the performance of centralized approach is not perfect in practice since it can only use connection request initial estimations. Any deviation from such estimations can lead to significant performance estimation. Furthermore, centralized solutions are inherently less scalable, due to the need to accumulate global network information either at a centralized entity or at each node. On the other hand, distributed spectrum management techniques are inherently more scalable and adept at dealing with traffic fluctuations and any unexpected changes in the network such as short or long term unavailability of links or spectrum bands. The performance of distributed spectrum assignment can be improved by adding more sophisticated priority based spectrum allocation schemes, such as the adaptive flag-based signaling scheme proposed in [32]. While we focus on the more generic performance comparison of centralized and distributed spectrum management algorithms in the current

study, we note that the practical performance of centralized algorithms is heavily dependent on strict knowledge of the traffic and network resources. We also note we use the busy-hour traffic in many of our simulation results in Sections 6 and 7. The performance of the distributed spectrum management approaches would improve under normal-hour traffic due to less spectrum contention.

3. EON and GMPLS Background

Figure 3 shows that the spectrum is divided into slices, or frequency slots (the term, “frequency slot” refers to a range of subcarrier frequencies.); i.e., they are separated into multiple subcarriers with their respective center frequencies. The slots have equal width, and the range of frequencies used by a slot is unavailable to other slots. The minimum *Slot Width Granularity* (SWG) is 12.5 GHz [5]. The slices are allocated around a center frequency and hence, the number of slices allocated for a slot must be even in number. The total bandwidth for a flexi-grid network is same as the WDM network, i.e., 4.4 THz. The numbers of subcarriers that are available are set at 352; that is, 352 frequency slots will be available at each link for the connections to traverse. As seen in Figure 4, the *Nominal Central Frequency Granularity* (NCFG) is the spacing between allowed nominal central frequencies and is set to 6.25 GHz. The slot width determines the “amount” of optical spectrum regardless of its actual “position” in the frequency axis.

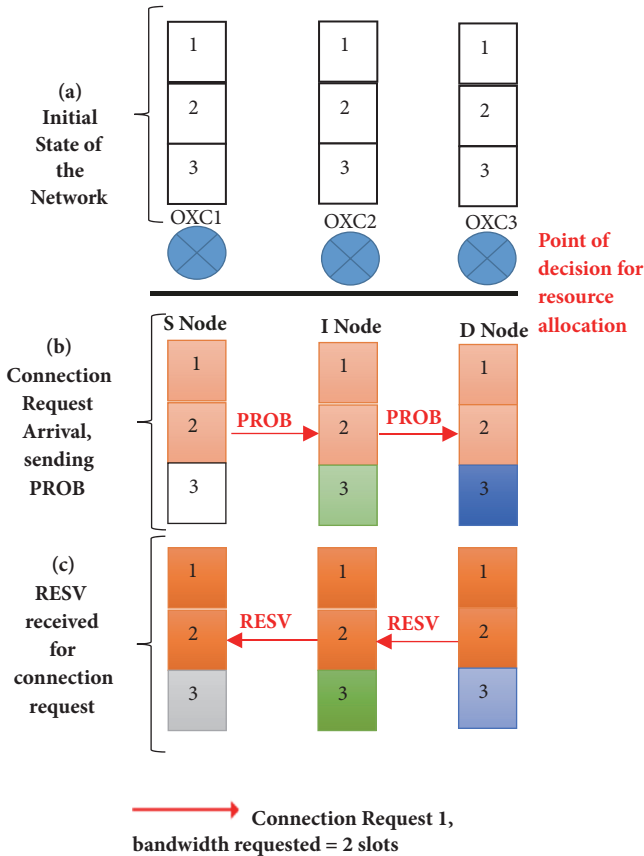


FIGURE 5: An illustration of the frequency slots in an EON being reserved using RSVP-TE-BRP signaling.

The set of nominal central frequencies can be built using the following expression: $f = 193.1 \text{ THz} + n \times 0.00625 \text{ THz}$, where 193.1 THz is the “anchor frequency” and n is an integer including zero. The *slot width* is constrained to be $m \times \text{SWG}$ (that is, $m \times 12.5 \text{ GHz}$), where m is an integer greater than or equal to unity [5].

FG-DWDM will divide the existing DWDM spectrum into smaller components that will require a mechanism for efficient spectrum resource allocation. There are two components to the problem of efficient spectrum resource allocation—(1) Signaling and (2) Routing and Spectrum Allocation (RSA). The control plane is the component of a routing device which interacts with its peers to exchange network state information. The control plane has several functions and, amongst them, its primary functions are *signaling and RSA*. In addition, it supports connection management by clients, provides protection and restoration services to the network and is responsible for tracking the conditions of the network topology, as well as for notifying the static or dynamic state of the network resources.

The *signaling* protocols work towards provisioning, managing, and deleting of connections. A resource reservation protocol is required for connection oriented optical networks. IP based networks focus on control protocols that are required to be periodically refreshed and polled throughout the network’s participating nodes. Today’s network designs

are largely based on a distributed architecture. Each element in the network maintains its state by exchanging its information base data via a distributed control. This kind of environment is usually seen in a standardized multivendor network deployment. GMPLS is used to resolve the challenges of a distributed control architecture where network elements can logically and dynamically exchange the information. The most fundamental service provided by the GMPLS control plane is dynamic end-to-end connection. The clients specify the parameters for connection requests and they are sent to the ingress node. GMPLS offers the following functionalities:

- (1) Resource discovery: saving state information of spectral resources and network nodes
- (2) Connection management: providing end-to-end service provisioning for a variety of services, such as connection creation, modification, and deletion.

In this paper, GMPLS is used as the underlying control plane in the simulator for the aforesaid reasons. Resource Reservation Protocol Traffic Engineering (RSVP-TE) is a signaling protocol used in-sync with GMPLS for resource reservation [18]. RSVP-TE can be used to reserve a lightpath wavelength if the wavelength that needs to be reserved is known in advance. The protocol has been modified for the simulations to incorporate wavelength selection algorithms. The signaling in RSVP takes place between the source and the destination node. Each intermediate node keeps a database of available resources before forwarding the request to the next node. In large scale networks, where there is a high volume of service requests, centralized control is not feasible for reasons such as delays in polling resource information base and control information propagation delay. Therefore, the usage of a distributed wavelength reservation protocol is essential. Realistic case studies [33] have been simulated for a network’s busy hour, with a lesser number of connection requests, in a near parallel mode to differentiate between the efficiency of Centralized Network Operation Mode (C-NOM) and (vs.) a Distributed Network Operation Mode (D-NOM). These case studies provide some optimal frequency, bandwidth, and base slot values [33] to achieve a 100% success rate in a centralized network operation during the busy hour of network state, which we utilize in this work. The two types of distributed reservation protocols that were used in simulations are Backward Reservation Protocol (BRP) and Forward Reservation Protocol (FRP). An illustration of BRP is described in Figure 5. The signaling packets used in FRP are

- (1) **RESV** reserves spectral resources temporarily
- (2) **CONF** confirms control packet that reserves the wavelength (or frequency slots) in the forward path
- (3) **FAIL** frees the temporarily reserved wavelengths and frees the connection from the network when spectral resources are unavailable;
- (4) **DROP** releases all the wavelengths after a certain hold time

Similarly, the signaling control packets used in BRP when the network state is in initial condition (Figure 5(a)) are

- (1) **PROB**: Passed from node to node, starting at the source node where a connection demand arrives and terminates at the destination node or an intermediate node (Figure 5(b))
- (2) **RESV**: A RESV packet is sent from the destination node to the source node for reserving the frequency slots once the PROB control packet has reached its destination by fulfilling the conditions of subcarrier contiguity and continuity (Figure 5(c))
- (3) **NACK**: A NACK request is sent and the connection is denied if the PROB request fails in between traversal from source to destination node, i.e., the spectral resources were not available
- (4) **DROP**: Releases all the wavelengths after a certain hold time

Figure 5 illustrates the methods by which slots are reserved in RSVP-TE-BRP signaling. Figure 5(a) shows that slots 1, 2, and 3 are available on every link of the network. In Figure 5(b), connection request 1 arrives and sends a PROB control packet requesting reservation (defined by First Fit RSA) of 2 bandwidth slots i.e., slots 1 and 2 in orange. Slot 3 at OXC2 and OXC3 is reserved by different connections—green and blue. PROB traverses the network to reach the destination (D) Node. PROB finds that slots 1 and 2 are available on each link; in Figure 5(c), a decision is made at the D-Node to send RESV control packet to source (S) Node and reserves the slots 1 and 2 (dark orange) while ignoring slot 3 at every link, which was occupied and probed by other requests.

4. Problem of Routing and Spectrum Allocation

Routing and Spectrum Allocation addresses the problem of computing contiguous blocks of frequency spectrum (or subcarriers) and the path to reach a request's destination [2, 4, 24]. Research in this area has been focused on dynamic RSA, which is broadly classified into centralized and distributed routing control. In centralized routing control, a global view of the network topology, spectrum resource availability (i.e., frequency slots), and physical impairment parameters (e.g., optical SNR, channel distortions), are maintained in the traffic engineering repository. In the distributed architecture the connections are provisioned by computing the signaling and spectrum allocation at individual nodes of the optical network. In distributed routing, each link, consisting of a pair of nodes, maintains its own network state information (i.e., network topology and available spectrum) and is collected in a local Traffic Engineering Database (TED) repository. Traditionally, the routing protocol (e.g., GMPLS OSPF-TE) is responsible for disseminating any changes occurring in the network state, thus allowing synchronization of all the nodes' TED repositories to have a unified view [34]. There have been several research papers that have proposed a distributed spectrum resource assignment approach for dynamic RSA in the GMPLS-enabled EONs [6]. In this paper's simulations, the RSA algorithms have been divided into two processes.

Path computation is performed as the first process as soon as a connection arrives with the information of source and destination. Then, based on the routing information obtained, network topology and resource information (i.e., the bandwidth required by the connection request) are collected dynamically for the traffic engineering database at every node, and spectrum resource assignment is performed at the destination node after traversing the complete path. For the complete signaling and resource allocation, the RSVP-TE FRP and BRP protocols are used to collect the subcarrier (frequency slot) availability information from every node in the path between the source and the destination.

Previous work on First Fit and Random Fit algorithms for WDM networks has been applied to Flex-grid network simulations [4]. When a connection requests some amount of bandwidth, it has to be in the form of contiguous blocks of frequency spectrum. The bandwidth is considered free if all the contiguous blocks are available. Let the bandwidth required be l and the starting slot or base slot is k . In a distributed architecture, the control packet first checks if the frequency slots from base-slot k to $k + l - 1$ are available i.e., if contiguous blocks of frequency are available by traversing from source to destination node. If the $k + l - 1$ slots are available within different ranges of spectrum, then the first such block of frequency spectra is selected. This spectrum allocation method is called the First Fit (FF) algorithm because the algorithm stops searching the spectrum database as soon as first free block of required bandwidth is found. Another algorithm to search the database of available subcarriers is the Random Fit (RF) algorithm. As the name of Random Fit suggests, the base slot is selected randomly while the bandwidth of connection is fixed. Figure 6 illustrates the two slot based algorithms. Slots are checked iteratively, defining a base slot i and looking ahead for n available consecutive slots assuming a sorted set, i.e.,

$$\text{spectrumSlot}[i] + n - 1 = \text{spectrumSlot}[i + n - 1]. \quad (1)$$

If a suitable range (i.e., base slot and bandwidth) is found, the base slot is reserved.

To summarize the algorithmic process, in the FF algorithm, the system selects the first available slot while in the RF algorithm, one base slot is randomly selected from a set of marked slots. All slot ranges containing a variable number (m) of free and consecutive slots are identified. The random policies are known to be inefficient because they create fragmentation in the optical spectra. In the FF policies, the chance of collision increases as connections compete near the vicinity of lower order range of spectra.

5. Simulation Environment

In this section, a centralized network operation is compared with respect to distributed network operation in the busy hour operation scenario for connection establishment. A specific set of 8 case studies is used for this comparative study [33] via the simulation tool for the results generated. The simulation tool has been completely developed in C++ and has a Graphical User Interface (GUI) to input specific

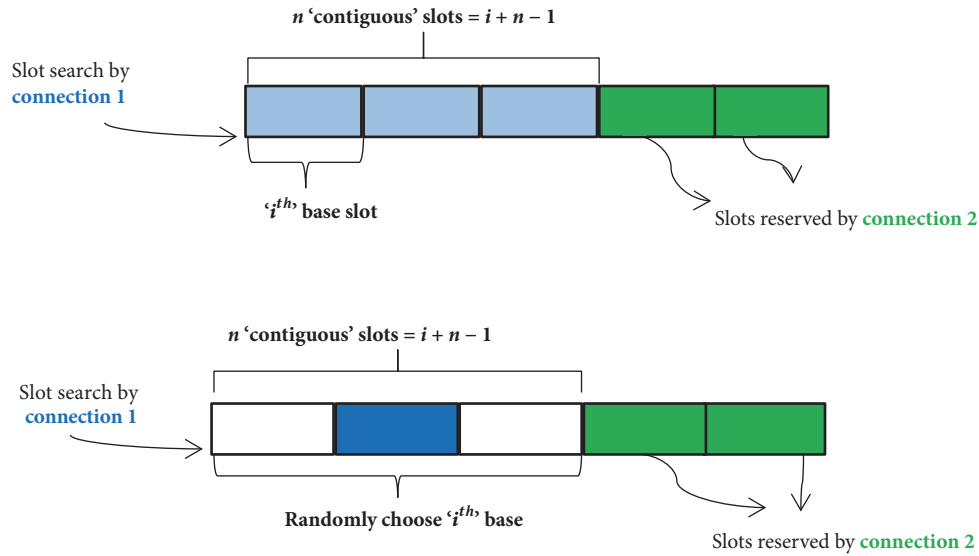


FIGURE 6: (a) First Fit Policy (FF): select the first free slot as the base slot; (b) random Fit (RF): identify slots of “m” range and select a base slot randomly.

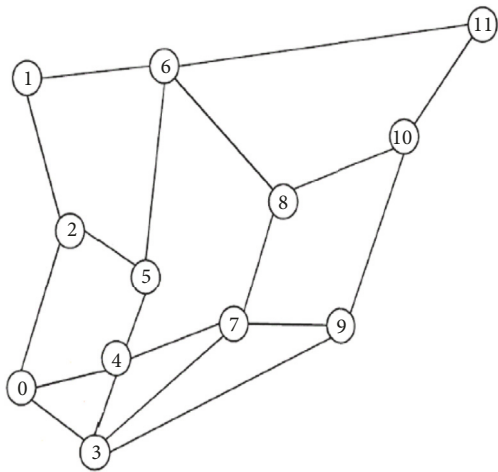


FIGURE 7: Finland topology with 12 nodes and 19 fiber links.

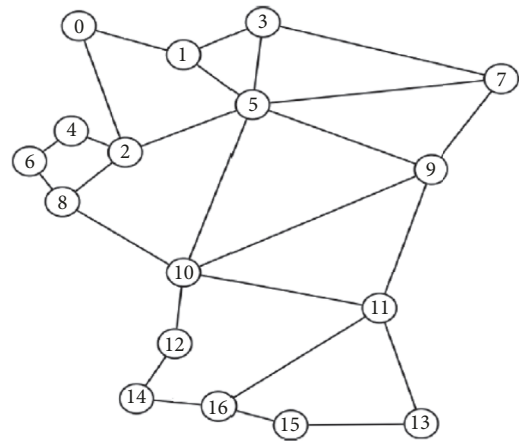


FIGURE 8: Germany topology with 17 nodes and 26 fiber links.

user defined network parameters. The following simulation results were generated by using a high arrival rate value (λ) of 1000 connections per second to emulate a parallel connection request arrival scenario. The service times were exponentially distributed. Each data point was obtained by averaging 10 consecutive simulation runs. Two different networks were used for the simulation, which are nationwide network scenarios: The Finland and Germany topologies were used as shown in Figures 7 and 8. The Finland network topology has 12 network nodes and 19 fiber links and the Germany network topology has 17 nodes and 26 fiber links. As in [33], which serves as the source of our 8 case studies for optimal capacity assignment, as well as many other EON studies, each link is assumed to have 160 frequency slots of 25 GHz (2x12.5 GHz), with a total spectrum capacity of 4 THz. As in many EON studies, we have not explicitly considered

guard bands in our simulations for simplicity. Though not significant in this research, it is noted that each link spans 5 km. In the centralized mode, the simulation tool utilizes predefined information from the case studies, namely, the source and destination node pair (ζ, δ), the bandwidth (θ), the frequency base slots (β), the (number of) hops (h), the path (ρ), and essentially uses control packet signaling. In the distributed mode only ζ, δ , and θ were used from the network configuration file to simulate similar scenarios by using the RSA algorithms and signaling. Table 1 describes the various events and parameters used in the simulations. The delay values for OXC and signal propagation are typically varied between milliseconds to microseconds [35]. The aforesaid parameters and values will be used, unless stated otherwise. In this paper, propagation delay on each link is assumed constant for simplicity.

TABLE I: Simulation events, control packets, delays, and delay values.

Events	FRP Messages	BRP Messages	Delays	Delay Values
Process	RESV	PROB	Tp = Packet processing delay at OXC	2 μ sec
Send	CONF	RESV	Tc = Configuration delay at OXC	10 μ sec
Config			Tl = Propagation Delay between each link	25 μ sec
Drop	FAIL	NACK	Tb = Data transmission duration	5 μ sec

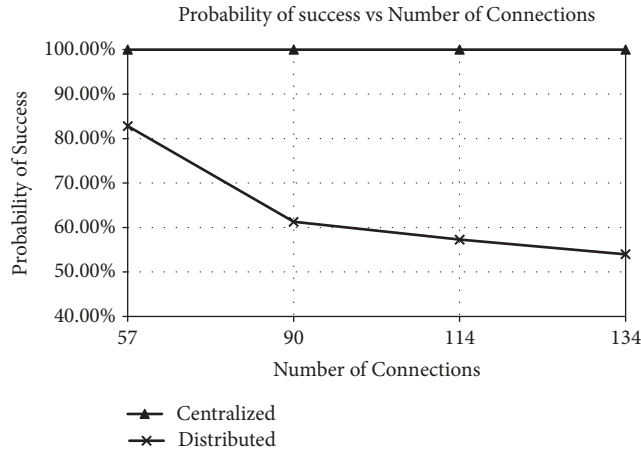


FIGURE 9: Probability of success vs number of connections in Finland topology.

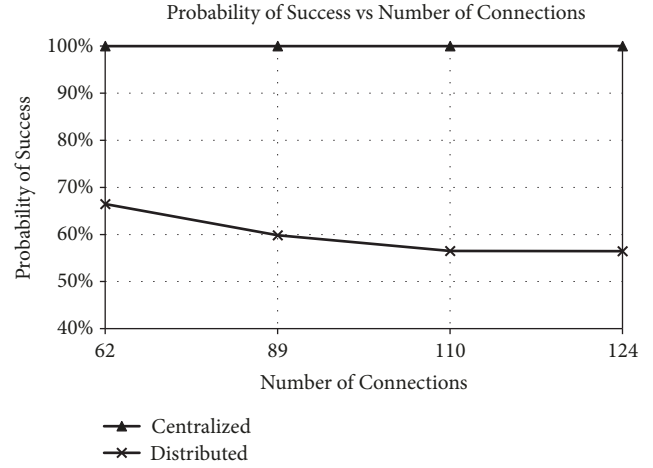


FIGURE 10: Probability of success vs number of connections in Germany topology.

6. Spectrum Allocation Comparisons

6.1. Forward Reservation Protocol: First Fit RSA with Parallel Arrivals. In this section, C-NOM and D-NOM are compared for the two different topologies chosen for analysis, namely, the Finland and Germany topologies. In all figures with y-axis representing delays, the delay is shown in seconds. In C-NOM results, it is assumed that spectrum assignment is centrally computed, and signaling is performed only to set up the paths. The first set of results is generated using the First Fit spectrum allocation algorithm. Figure 9 shows the Probability of Success vs. Number of Connections for the Finland topology in a comparison between a centralized and distributed network operation mode. The probability of success is maintained at 100% even when the number of connections arriving in parallel is increased using C-NOM, because a network operator had all the network state information prior to busy hour. Thus, the simulation produced a 100% success rate, as expected. On the contrary, when using D-NOM, the probability of success drops sharply as the number of parallel connection arrivals is increased, with a difference of 20% or higher, because there is no predefined optimization. The values of β and ρ are found by the FF RSA algorithm. A similar trend was observed in the Germany topology as shown in Figure 10. The probability of success is always 100% in this scenario, too, for all the parallel arrivals. There is a 30% and larger difference in probability of success, between C-NOM and D-NOM.

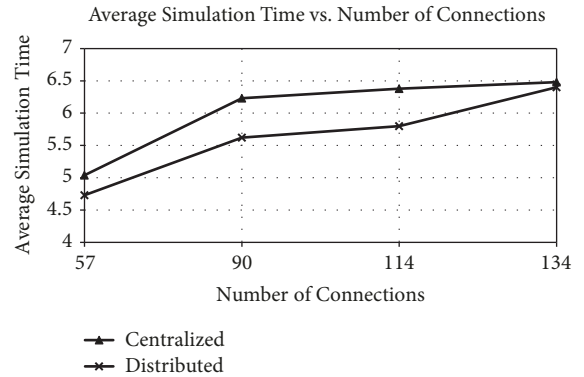


FIGURE 11: Average connection established time vs number connections in Finland topology.

A key performance metric, *the average connection established time*, denoting how long it takes, on average, to set up a successful connection request, is now discussed. Average connection established time vs. Number of Connections, for C-NOM and D-NOM comparison, is seen in Figure 11.

From Figure 11, in the Finland topology, it can be observed that the average connection established time of D-NOM is lower than the C-NOM, because there were a larger number of failed connection set up attempts and a fewer number of events to execute in D-NOM. There is a trend of increasing average connection established time in both scenarios. This behavior was confirmed by examining the

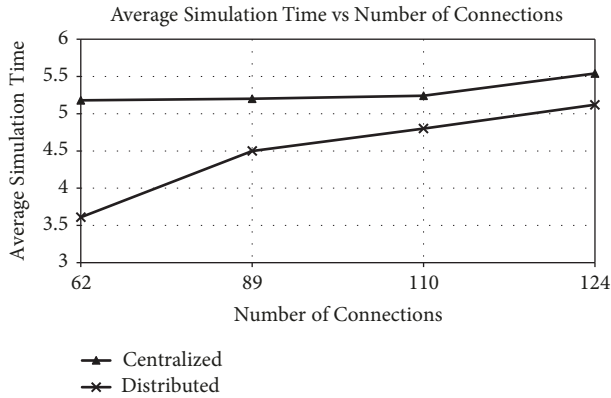


FIGURE 12: Average connection established time vs number of connections in Germany topology.

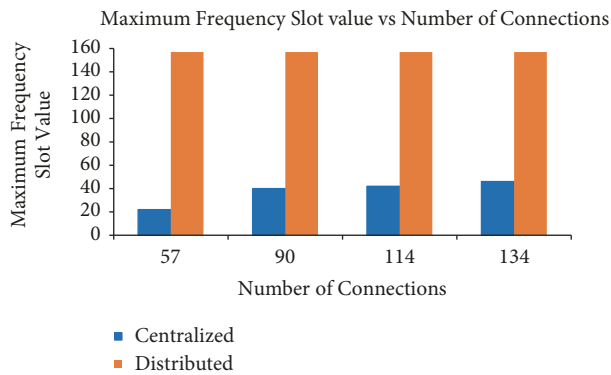


FIGURE 13: Max frequency slot value vs number of connections in Finland topology.

average number of events executed for the C-NOM and D-NOM scenarios. In Figure 12, it is observed that the average connection established time for the Germany topology, where the average time for C-NOM is greater than D-NOM. Although the connection established time of C-NOM took longer than D-NOM by 0.5 to 1.5 seconds (depending on the number of connection arrivals), it guaranteed a 100% success in connection service.

To understand the resource allocation in D-NOM and C-NOM, the maximum assigned frequency slot value was collected. The maximum slot value is the highest value of frequency slot that was used by a connection for its (ζ, δ) pair in the complete network. This is displayed in Figures 13 and 14.

From Figures 13 and 14, it can be observed that the maximum frequency slot used in C-NOM is in the lower order of the spectrum. A total of 160 frequency slots are used per fiber with each slot's width equal to 25 GHz. In the highest parallel arrival case of 134 parallel arrivals, the maximum slot value used is 54. So, if C-NOM is efficiently used, then a larger number of connection requests can be accommodated in the network. On the other hand, when D-NOM is used, the requests face contention in the lower band of spectrum. This results in a larger failure rate because each connection tries to reserve a higher order frequency slot, using the first

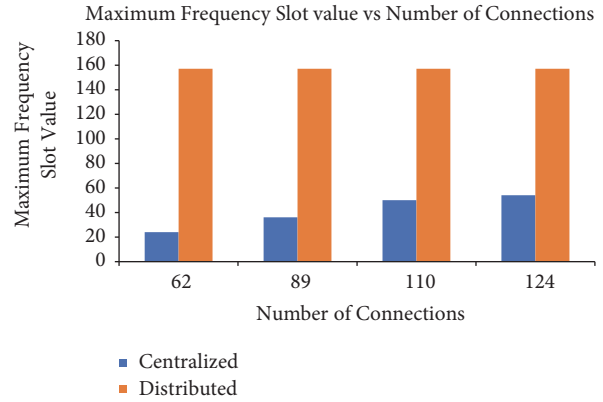


FIGURE 14: Maximum frequency slot value vs number of connections in Germany topology.

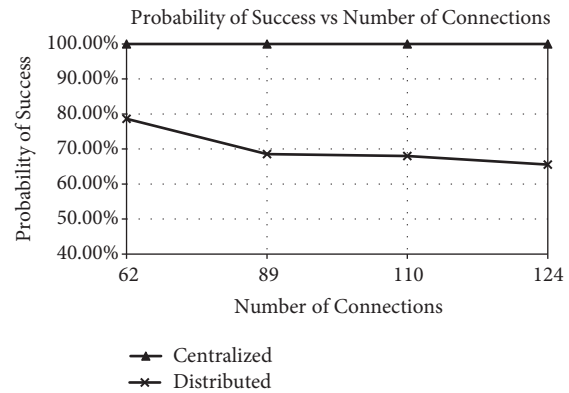


FIGURE 15: Probability of success vs number of connections in Germany topology.

fit algorithm, as the number of connections increase within the network.

Connections using the first fit methodology in D-NOM always try to utilize all the available resources and reserve the slots in the higher order of the spectrum. From the simulations, it was observed that maximum slot value being reserved is 157.

6.2. Backward Reservation Protocol: First Fit RSA with Parallel Arrivals. This section covers the BRP signaling in C-NOM and D-NOM. Again, the data that has been used in C-NOM, i.e., ζ , δ , β , θ , h , and ρ , have been referred from realistic network case studies [33]. The simulation parameters are the same as in Table 1. In this section only the Germany topology is considered.

In Figure 15, it can be observed that the probability of success for C-NOM is 100%, because predefined and optimized data were used. However, in D-NOM, the value of β , h , and ρ are found by the FF RSA algorithm and may not be the optimum value.

Figure 16 displays the average connection established time versus the number of connections in the Germany topology. From Figure 16, it can be observed that the

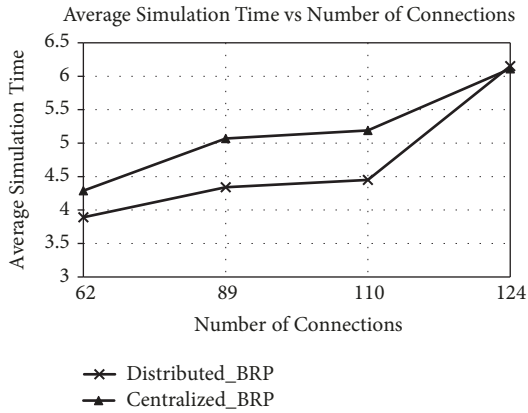


FIGURE 16: Average connection established time vs number of connections in Germany topology.

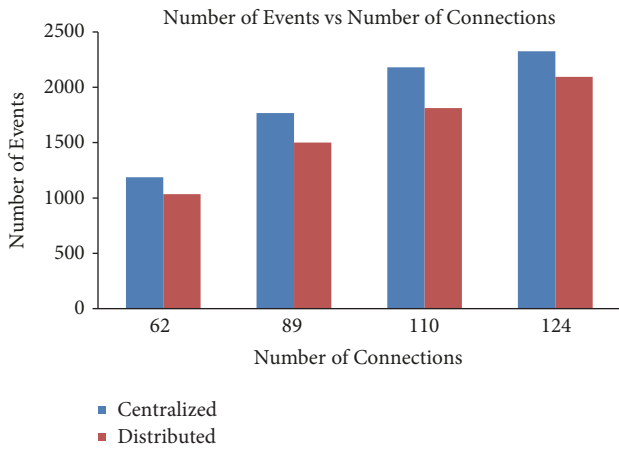


FIGURE 17: Number of events vs number of connections in Germany topology.

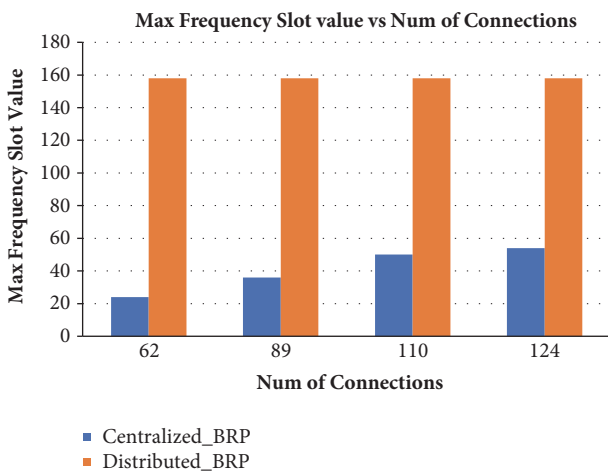


FIGURE 18: Maximum frequency slot value vs number of connections in Germany topology.

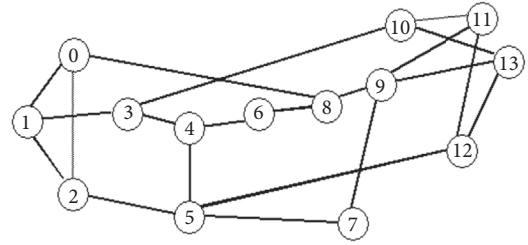


FIGURE 19: 14 node NSFNET topology.

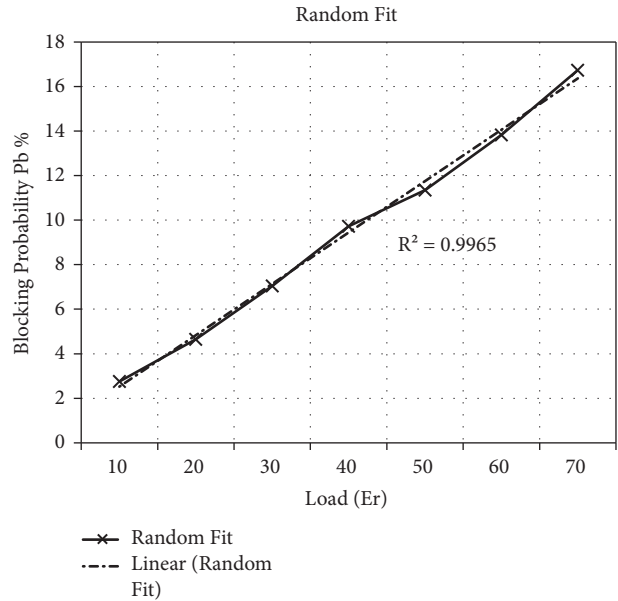


FIGURE 20: Random Fit with BRP and Poisson arrivals.

connection established time for D-NOM is lower than the C-NOM system. As the numbers of connections are increased, the connection established time also increases. Since there are failed attempts in D-NOM, connection established time is lower than that of the C-NOM approach. This is reconfirmed in Figure 17.

From Figure 17, the numbers of events in D-NOM are lower than C-NOM for all numbers of connections. Naturally, the numbers of events increase as the number of connections being simulated are increased.

From the simulations, it was observed that the maximum frequency slot that was used on a link for a particular (ζ, δ) pair in the complete network is 158 in D-NOM system. The FF algorithm searches for every base slot available; this implies that a distributed system is inefficiently allocating frequency slots and, so, the blocking of connection requests will increase as the numbers of connections are increased.

In C-NOM, the optimized values of slots to be used are already known, so the maximum frequency slot used is 54. This means more connections can be accommodated in the network. The results can be observed in Figure 18.

Comparing the results of C-NOM and D-NOM in terms of frequency slot allocation, it can be observed that C-NOM

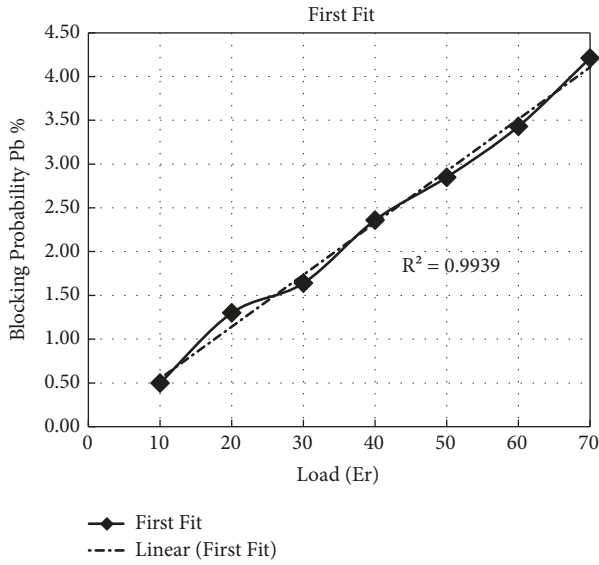


FIGURE 21: First Fit with BRP and Poisson arrivals.

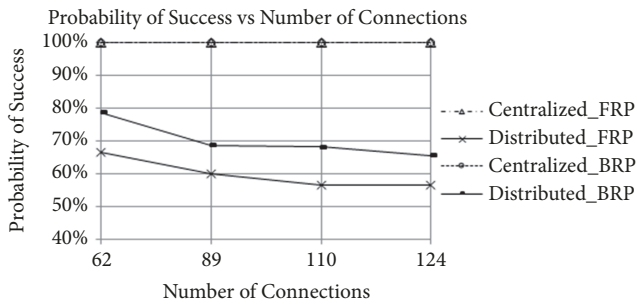


FIGURE 22: Probability of success for C-NOM and D-NOM using FRP and BRP with parallel arrivals.

TABLE 2: Simulation setup.

Parameter	Value
Number of frequency slots	352
Number of nodes in the network	14
Number of connections	8000
Slot Allocation	Uniform Dist.[1,4]
Connection Distribution	Uniform Dist.[1,14]
Exponential Service Rate	1
Poisson Arrivals	
Number of simulated runs	10

uses the lower order spectrum efficiently and even saves spectrum for accommodating more connection requests. D-NOM uses the lower order spectrum like C-NOM but fails to accommodate as many connections as C-NOM, using FF.

6.3. First Fit and Random Fit RSA with Poisson Arrivals. In this section, stochastic traffic arrival is used as compared to parallel arrivals in previous sections. Table 2 displays the parameters that are used for the simulation setup.

The event delays are in microseconds and Poisson arrival rates were simulated. The topology used is the 14 node NSFNET topology, shown in Figure 19.

It can be observed from Figures 20 and 21 that first fit algorithm performs better than the random fit algorithm in terms of blocking probability, as might be expected due to more efficient packing of the available frequency slots, with little fragmentation. As the arrival rate is increased, the blocking probability also increases with a linear rate in both cases, as shown with the corresponding linear fitting in each figure.

7. Comparison between FRP and BRP

In this section, as a summary, various metrics are compared when FRP and BRP signaling methods are used in simulations with different network modes and traffic arrivals in the Germany topology. The results can be intuitively understood as they follow a heuristic approach and rely on the simulations.

In Figure 22, the probability of success can be observed for C-NOM and D-NOM with both signaling methods in the Germany topology. The performance of BRP is better in D-NOM because the resources are not temporarily reserved in the path; rather, they are probed for availability and permanently reserved when a control message is sent from a destination node towards a source node. There is almost a difference of 10% in FRP and BRP when D-NOM scenario is simulated.

The best approach for parallel arrivals while using any signaling technique is C-NOM. The centralized approach works effectively because the network operator knows *a priori* that the network congestion can be resolved at a particular traffic rate by statically designating routes, bandwidth, and frequency base slots.

Figure 23 demonstrates the average connection established time taken by a successful connection. The C-NOM scenario for BRP takes the longest time because of two reasons:

- (1) All the connections were successful, which infers maximum events were simulated;
- (2) BRP signaling carries more signaling time overhead because of backward reservation.

The C-NOM scenario for FRP takes the least time because all the connections are reserved in the forward path which results in less signaling time overhead. The D-NOM approach of BRP and FRP have a very low margin of difference because, in both cases, the RSA algorithm must search for base slots and failures reduce the number of events, inferring less signaling delays.

The maximum frequency slot allocation metric is an important aspect in busy hour traffic simulation, because an early exhaustion of slots results in higher connection blocking. By using the first fit algorithm in simulations, it was observed that the D-NOM approach tries to utilize the complete band of 4 THz, with a high contention in the lower band of the spectrum, resulting in failed attempts. In D-NOM, BRP and FRP have unequal amounts of maximum

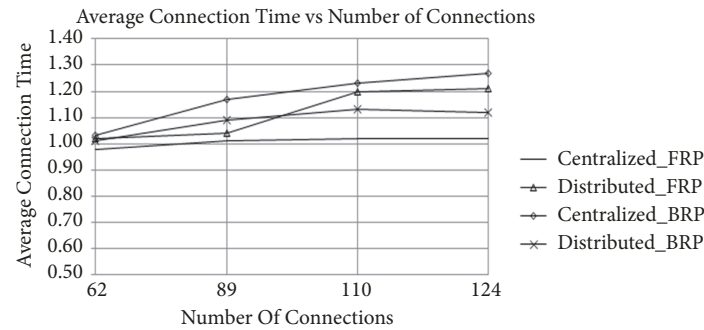


FIGURE 23: Average connection established time for C-NOM and D-NOM using FRP and BRP with parallel arrivals.

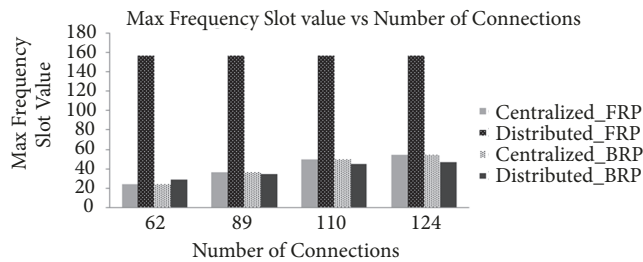


FIGURE 24: Maximum frequency slot value for C-NOM and D-NOM using FRP and BRP.

spectrum slot allocation. In the FRP simulation, the highest slot reserved was observed to be the 157th, while in BRP the high slot reserved was the 47th slot (Figure 24), when using FF.

The comparative study of C-NOM and D-NOM (using FF algorithm) systems for parallel or busy hour traffic, with FRP and BRP signaling techniques, illustrates that the C-NOM system performs better than the D-NOM system in terms of efficient frequency slot allocation, average connection established time and probability of success.

In the normal hours of operation, the connections arriving in the network are modeled with an exponential distribution of arrival time; i.e., no two connections arrive at the same time. It can be observed, in the study, that the D-NOM system's relative blocking performance improves when the traffic is in the stochastic state (Figure 21) as opposed to parallel arrivals under BRP and FF algorithm, due to less resource contention.

From the aforementioned results and their respective comprehension, the C-NOM system can be employed by a network operator when the network state is approaching busy hour traffic, with BRP signaling. From Figure 23, it can be observed that the average connection established time is the lowest for C-NOM. During the normal network operation hours, a D-NOM approach is efficient in allocating resources dynamically, using the FF algorithm, as the network state changes constantly, using the BRP signaling as seen in Figure 24. The simulation tool which is used in this modeling can be used in future to develop mixed models for parallel and stochastic network traffic arrivals and service. This will enable a network operator to dynamically assess the situation

and use the C-NOM and D-NOM system with BRP signaling accordingly.

8. Conclusion

A detailed simulator was developed and a comprehensive performance evaluation of various centralized and distributed GMPLS-based connection establishment approaches in flex-grid elastic optical networks was carried out. It was demonstrated that C-NOM performs better than D-NOM when traffic is generated in the busy hour of the network, i.e., in the case of parallel arrival of connections. The study of C-NOM and D-NOM, for busy hour traffic, demonstrates that C-NOM systems have a 100% probability of success. The average connection established time analysis shows that FRP is faster than BRP to achieve 100% success in C-NOM with parallel arrival simulation. It has also been demonstrated that BRP signaling helps in obtaining better performance than FRP signaling for D-NOM during normal hours of network operation.

Data Availability

The data used to support the findings of this study are available from the authors upon request.

Conflicts of Interest

The authors declare that there are no conflicts of interest regarding the publication of this paper.

References

- [1] G. Zhang, M. De Leenheer, A. Morea, and B. Mukherjee, "A survey on ofdm-based elastic core optical networking," *IEEE Communications Surveys & Tutorials*, vol. 15, no. 1, pp. 65–87, 2013.
- [2] B. C. Chatterjee, S. Ba, and E. Oki, "Fragmentation problems and management approaches in elastic optical networks: a survey," *IEEE Communications Surveys & Tutorials*, vol. 20, no. 1, pp. 183–210, 2018.
- [3] M. Jinno, H. Takara, and B. Kozicki, "Concept and enabling technologies of spectrum-sliced elastic optical path network (SLICE)," in *Proceedings of the 2009 Asia Communications*

- and Photonics Conference and Exhibition, ACP 2009, pp. 1-2, Shanghai, China, November 2009.
- [4] S. Talebi, F. Alam, I. Katib, M. Khamis, R. Salama, and G. N. Rouskas, "Spectrum management techniques for elastic optical networks: A survey," *Optical Switching and Networking Journal*, vol. 13, pp. 34–48, 2014.
 - [5] "Spectral grids for WDM applications: DWDM frequency grid," ITU-T Recommendation G.694.1, November 2012.
 - [6] T. Fukuda, L. Liu, K.-I. Baba, S. Shimojo, and S. J. B. Yoo, "GMPLS control plane with distributed multipath RMSA for elastic optical networks," *Journal of Lightwave Technology*, vol. 33, no. 8, pp. 1522–1530, 2015.
 - [7] D. T. Hai, M. Morvan, and P. Gravey, "Combining heuristic and exact approaches for solving the routing and spectrum assignment problem," *IET Optoelectronics*, vol. 12, no. 2, pp. 65–72, 2018.
 - [8] W. Zheng, Y. Jin, W. Sun, W. Guo, and W. Hu, "On the spectrum-efficiency of bandwidth-variable optical ofdm transport networks," in *Proceedings of the Optical Fiber Communication Conference*, San Diego, Calif, USA, 2010.
 - [9] X. Wan, L. Wang, N. Hua, H. Zhang, and X. Zheng, "Dynamic routing and spectrum assignment in flexible optical path networks," in *Proceedings of the National Fiber Optic Engineers Conference, NFOEC 2011*, pp. 1–3, Los Angeles, CA, USA, March 2011.
 - [10] T. Takagi, H. Hasegawa, K. Sato et al., "Algorithms for maximizing spectrum efficiency in elastic optical path networks that adopt distance adaptive modulation," in *Proceedings of the 2010 36th European Conference and Exhibition on Optical Communication - (ECOC 2010)*, pp. 1–3, Torino, Italy, September 2010.
 - [11] R. Muñoz, R. Casellas, and R. Martínez, "Dynamic distributed spectrum allocation in gmpls-controlled elastic optical networks," in *Proceedings of the European Conference and Exposition on Optical Communications*, pp. 1–3, Geneva, Switzerland, 2011.
 - [12] Z. Zhu, W. Lu, L. Zhang, and N. Ansari, "Dynamic service provisioning in elastic optical networks with hybrid single-/multi-path routing," *Journal of Lightwave Technology*, vol. 31, no. 1, pp. 15–22, 2013.
 - [13] A. Horota, L. Reis, G. Figueiredo, and N. L. S. Da Fonseca, "Routing and spectrum assignment algorithm with most fragmented path first in elastic optical networks," in *Proceedings of the 7th IEEE Latin-American Conference on Communications, LATINCOM 2015*, pp. 1–6, Arequipa, Peru, November 2015.
 - [14] F. Palmieri, "GMPLS control plane services in the next-generation optical internet," *The Internet Protocol Journal*, vol. 11, no. 3, 2011.
 - [15] K. Christodouloupoulos, I. Tomkos, and E. A. Varvarigos, "Routing and spectrum allocation in OFDM-based optical networks with elastic bandwidth allocation," in *Proceedings of IEEE Globecom*, Miami, FL, USA, December 2010.
 - [16] L. Velasco, A. Castro, M. Ruiz, and G. Junyent, "Solving routing and spectrum allocation related optimization problems: from off-line to in-operation flexgrid network planning," *Journal of Lightwave Technology*, vol. 32, no. 16, pp. 2780–2795, 2014.
 - [17] Y. Xiaosong, Y. Zhao, J. Zhang, B. Mukherjee, J. J. Zhang, and X. Wang, "Static routing and spectrum assignment in co-existing fixed/flex grid optical networks," in *Proceedings of the Optical Fiber Communications Conference and Exhibition (OFC)*, pp. 1–3, 2014.
 - [18] L. Berger, "Generalized multi-protocol label switching (gmpls) signaling resource reservation protocol-traffic engineering (RSVP-TE) extensions," RFC 3473, January 2003.
 - [19] G. Sahin, S. Subramaniam, and M. Azizoglu, "Signaling and capacity assignment for mesh-based restoration schemes in optical networks," *Journal of Optical Networking*, vol. 1, no. 5, pp. 188–205, 2002.
 - [20] R. D. Doverspike, G. Sahin, J. L. Strand, and R. W. Tkach, "Fast restoration in a mesh network of optical cross-connects," in *Proceedings of the Optical Fiber Communication Conference*, 1999.
 - [21] X. Zhang, L. Guo, W. Hou et al., "Experimental demonstration of an intelligent control plane with proactive spectrum defragmentation in SD-EONs," *Optics Express*, vol. 25, no. 20, pp. 24837–24852, 2017.
 - [22] B. C. Chatterjee, T. Sato, and E. Oki, "Recent research progress on spectrum management approaches in software-defined elastic optical networks," *Optical Switching and Networking*, vol. 30, pp. 93–104, 2018.
 - [23] A. Sadasivarao, D. Naik, C. Liou, S. Syed, and A. Sharma, "Demystifying SDN for optical transport networks: Real-world deployments and insights," in *Proceedings of the 59th IEEE Global Communications Conference, GLOBECOM 2016*, Washington, DC, USA, December 2016.
 - [24] B. C. Chatterjee, N. Sarma, and E. Oki, "Routing and spectrum allocation in elastic optical networks: a tutorial," *IEEE Communications Surveys & Tutorials*, vol. 17, no. 3, pp. 1776–1800, 2015.
 - [25] O. Gerstel, M. Jinno, A. Lord, and S. J. B. Yoo, "Elastic optical networking: a new dawn for the optical layer?" *IEEE Communications Magazine*, vol. 50, no. 2, pp. S12–S20, 2012.
 - [26] M. Klinkowski and K. Walkowiak, "Routing and spectrum assignment in spectrum sliced elastic optical path network," *IEEE Communications Letters*, vol. 15, no. 8, pp. 884–886, 2011.
 - [27] M. Jinno, B. Kozicki, H. Takara et al., "Distance-adaptive spectrum resource allocation in spectrum-sliced elastic optical path network [Topics in Optical Communications]," *IEEE Communications Magazine*, vol. 48, no. 8, pp. 138–145, 2010.
 - [28] V. López and L. Velasco, *Elastic Optical Networks: Architectures, Technologies, and Control*, Springer International Publication Switzerland, 2016.
 - [29] S. Ba, B. C. Chatterjee, and E. Oki, "Defragmentation scheme based on exchanging primary and backup paths in 1+1 path protected elastic optical networks," *IEEE/ACM Transactions on Networking*, vol. 25, no. 3, pp. 1717–1731, 2017.
 - [30] S. K. Routray, G. Sahin, J. R. F. Da Rocha, and A. N. Pinto, "Statistical analysis and modeling of shortest path lengths in optical transport networks," *Journal of Lightwave Technology*, vol. 33, no. 13, pp. 2791–2801, 2015.
 - [31] T. Mathur, *Study of spectrum allocation schemes in Generalized Multi Protocol Label Switched Control Plane Enabled Flexi Grid Networks [Master thesis]*, Computational Electrical and Computer Eng. Thesis, Miami University, 2015.
 - [32] A. Albaidhani, G. Sahin, and D. Ucci, "Adaptive flag-based signaling for distributed spectrum assignment spectrum assignment in elastic optical networks," in *Proceedings of the IFIP/IEEE International Conference on Network and Service Management*, 2018.
 - [33] A. de Sousa, C. B. Lopes, and P. Monteiro, "Design cost and spectrum efficiency comparison of fixed-grid and flex-grid optical networks with grooming," in *Proceedings of the 2014 16th International Telecommunications Network Strategy and*

Planning Symposium (NETWORKS), pp. 1–4, Funchal, Portugal, September 2014.

- [34] X. Yuan, R. Gupta, and R. Melhem, “Distributed control in optical WDM networks,” in *Proceedings of the Military Communications Conference, MILCOM '96*, IEEE, McLean, VA, USA, 1996.
- [35] L. Xin and M. Hamdi, “On scheduling optical packet switches with reconfiguration delay,” *IEEE Journal on Selected Areas in Communications*, vol. 21, no. 7, pp. 1156–1164, 2003.

